Projected Changes in Flood and Drought Risks Under Climate Change in the 21st Century: A Multi-GCM Multi-GHM Approach

Behzad Asadieh[1*], Nir Y. Krakauer[2]

[1,2] *Civil Engineering Department and NOAA-CREST, The City College of the City University of New York - Correspondence at * basadie00@citymail.cuny.edu*

Abstract

Global warming is expected to intensify the Earth's hydrological cycle with increased flood and drought risks. We analyze changes in global daily streamflow extremes for the 20th and 21st centuries under two different warming scenarios, using an ensemble of bias-corrected global climate model fields fed into different hydrological models. Analysis of multi-model mean changes in high and low streamflow percentiles reveals that approximately 37 and 43% of the global land areas are exposed to increases in flood and drought risks, respectively, by the end of the 21st century. Nearly 10% of the global land areas are under the potential threat of simultaneous increase in flood and drought risks; unfortunately, these regions tend to be highly populated parts of the globe, currently holding around 30% of the world's population (more than 2.1 billion people). In a world more than 4 degrees warmer by the end of the 21st century compared to the pre-industrial era (RCP8.5 scenario), flood and drought events are projected to be more intense than in a nearly 2 degree warmer world (RCP2.6 scenario). In both scenarios, models with high certainty project significant increases in streamflow of the regions near and above the Arctic Circle, and consequent increases in the freshwater inflow to the Arctic Ocean, while subtropical arid areas experience further reduction in streamflow.

Materials and Methods

We use daily streamflow simulations from 25 GCM-GHM combinations (5 GCMs and 5 GHMs) from the Inter-Sectoral Impact Model Intercomparison Project (ISI-MIP). We analyze simulated streamflow of the end of the 21st century (2070-2099, 21C) in comparison with the end of the 20th century (1971-2000, 20C). We study changes in the magnitude of the 95th percentile of annual streamflow (P95) in 21C compared to 20C, in which an increase would be an indication of increase in the flooding risk. We also study the change in the magnitude of the 5th percentile (P5), in which a decrease would correspond to an increase in the drought risk. We study both low and high radiative forcing scenarios (RCP2.6 and RCP8.5) to investigate the impacts of 21C anthropogenic forcing on flood and drought risk.

The first fast-track phase of the ISI-MIP presents bias-corrected outputs from the following 5 GCMs: GFDL-ESM2M, HadGEM2-ES, IPSL-CM5A-LR, MIROC-ESM-CHEM and NorESM1-M. The 5 selected GHMs for this study are: WBM, MacPDM, PCR-GLOBWB, DBH and LPJmL. ISI-MIP provides the outputs for only 5 GCMs, from more than 5 GHMs. Here, the number of GHMs is also limited to 5 so that the uncertainties arising from the GCMs and GHMs are readily comparable.

Changes are normalized to between -1 and +1. Increase in the magnitude of P95 indicates increase in flooding risk. Since increased drought risk corresponds to decrease in the magnitude of P5, the normalized changes in P5 are multiplied by -1, to form the drought risk indicator. We refer to positive/negative normalized change in P95 (P5) as increased/decreased flood (drought) risk, respectively. Averaged normalized changes are reverted to relative changes and results are shown in both normalized and relative percentages.

In order to calculate the normalized change in flood risk of a grid cell, the magnitude of the 95th percentile of annual streamflow (P95) is calculated for each year, and then averaged for 20C (called Q20C) and 21C (called Q21C). The normalized change is calculated as:

$$\Delta Q = \frac{Q_{21C} - Q_{20C}}{Q_{21C} + Q_{20C}}$$

The ΔQ value ranges between -1 and +1, where a normalized change equal to -1 indicates total loss of the 20C flow in the 21C and a normalized change equal to +1 indicates that all the 21C flow is resultant of the change and the flow in 20C was zero. For normalized change in drought risk of a grid cell, the same calculations are performed on the magnitude of the 5th percentile of annual streamflow (P5) and the ΔQ is multiplied by -1 so a positive number would indicate increase in drought (decrease in low flow). The normalized changes are multiplied by 100 afterwards to be presented as percentages. The normalized change percentages are shown in the text as well as reverted values to the relative change percentages.

Dry grid cells with average flow of less than 0.01 mm/day for 1971-2000 period (using the WBM-plus hydrological model driven by observation-based WFD climate data), as well as Greenland and Antarctica, are excluded from the calculations. The remaining grid cells, studied in the present paper, cover 75.9% of global land area, but include 95.9% of global population as of the year 2015.

Increase and decrease in flood and drought can form the four combinations, which are categorized as the following four quadrants: 1. Increased flood and decreased drought, 2. Increased flood and drought, 3. Increased drought and decreased flood and 4. Decreased flood and drought. Assignment of each grid cell to the specified quadrants is based on the averaged normalized change across GCMs and GHMs. Results obtained are averaged for each of these quadrants and the comparison of results between different scenarios is made for each quadrant individually.

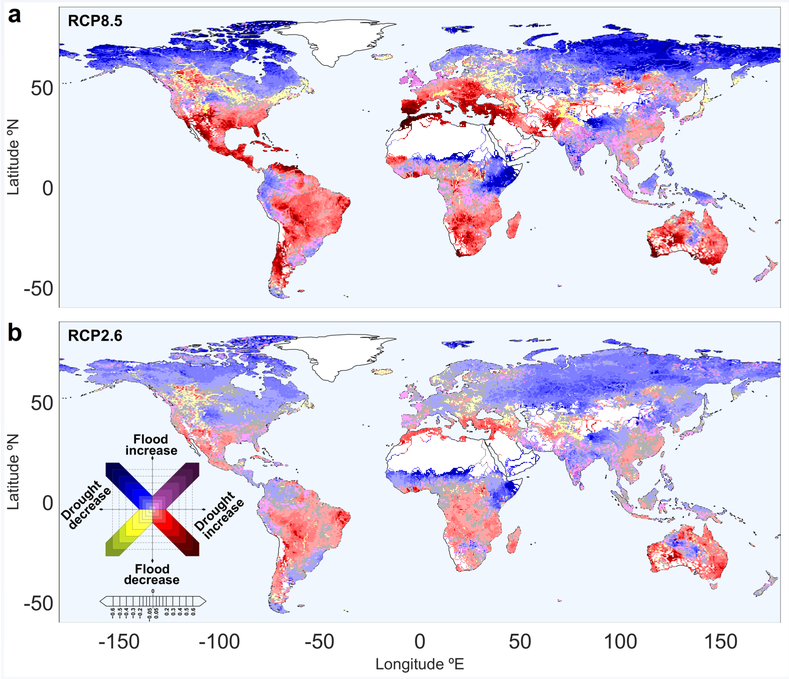

Figure 1 | Global distribution of change in flood and drought indicators. a, under RCP8.5 scenario and **b,** under RCP2.6 scenario. Grid cells with increased flood (Quad. 1) and drought (Quad. 2) are shown in blue and red shades, cells with increase in both flood and drought (Quad. 3) are shown in purple shade and cells with decrease in both flood and drought (Quad. 4) are shown in yellow shade. The saturation of colors show the intensity of change. Grid cells with normalized changes less than 1% (equal to 2% in relative terms) are considered as no change cells and are shown in gray.

Table 1: Normalized change in high and low streamflow averaged for each quadrant (normalized %). The numbers in parenthesis show the changes reverted to the relative terms (relative %).

	Quad. 1. flood increased		Quad. 2. flood and drought increased		Quad. 3. drought increased		Quad. 4. flood and drought decreased	
	Change in flood	Change in drought	Change in flood	Change in drought	Change in flood	Change in drought	Change in flood	Change in drought
RCP 8.5	13.11% (30.20% rel.)	-19.09% (-32.05% rel.)	4.81% (10.10% rel.)	9.01% (19.80% rel.)	-12.90% (-22.85% rel.)	23.72% (62.20% rel.)	-5.08% (-9.65% rel.)	-11.83% (-21.15% rel.)
RCP 2.6	7.00% (15.05% rel.)	-10.74% (-19.40% rel.)	3.06% (6.30% rel.)	5.56% (11.80% rel.)	-5.93% (-11.20% rel.)	12.30% (28.05% rel.)	-2.67% (-5.20% rel.)	-6.35% (-11.95% rel.)

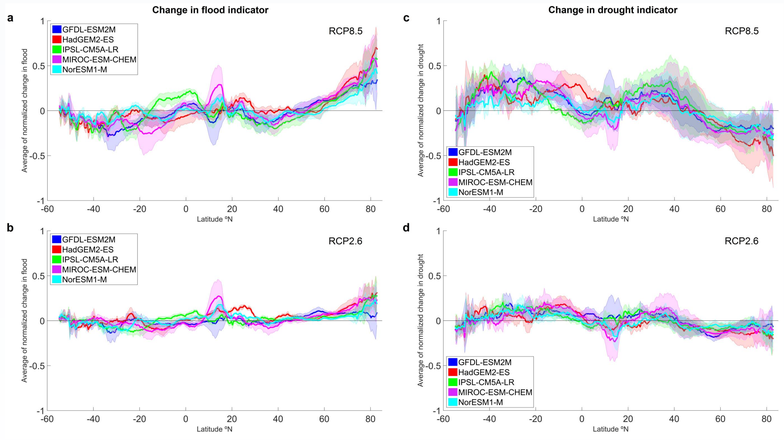

Figure 2 | Change in flood indicator under RCP8.5 (a) and RCP2.6 (b) scenarios and change in drought indicator under RCP8.5 (c) and RCP2.6 (d) scenarios, averaged by latitude. The thick lines in the plots show the mean change in the streamflow of each GCM routed by multiple GHMs, and the shades denote ±1 st. dev. The plots show that routings of a single GCM form various GHMs yield different results.

Table 2: Percent of population and land area affected by each flood and drought risk change quadrant, for RCP 2.6 and RCP 8.5 radiative forcing scenarios. Percentages are from the population and area studied, and not from the global totals. However, the 75.9% of global land area studied is home to 95.9% of total global population in the year 2015.

		Quad. 1. Flood increase, drought decrease	Quad. 2. Flood and drought increase	Quad. 3. Drought increased, flood decrease	Quad. 4. Flood and drought decrease	Flood Increase (Sum of Quads. 1 and 2)	Drought Increase (Sum of Quads. 3 and 2)
Land area affected (% of 113 million km^2 studied)	RCP 8.5	35.6%	12.7%	44.3%	7.4%	48.3%	56.9%
	RCP 2.6	45.5%	14.3%	33.6%	6.6%	59.8%	47.9%
Population affected (% of 6.84 billion people studied)	RCP 8.5	25.1%	30.9%	39.8%	4.2%	56.0%	70.7%
	RCP 2.6	37.1%	28.3%	30.1%	4.5%	65.4%	58.5%

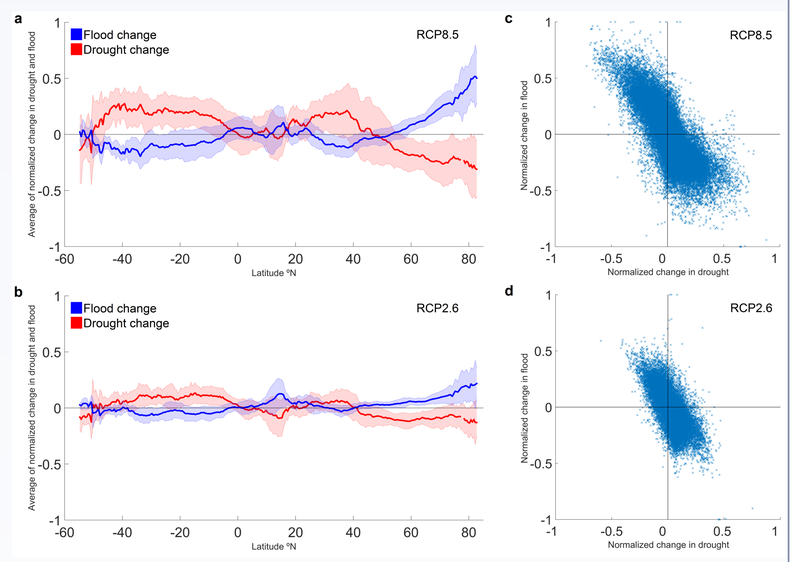

Figure 3 | Change in flood and drought indicators under RCP8.5 (a) and RCP2.6 (b) scenarios, averaged by latitude. Scatter plot of change in flood and drought indicator for each grid cell under RCP8.5 (c) and RCP2.6 (d) scenarios. The thick line in the plots show the ensemble mean of all 25 GCM-GHM combinations and the shades denote ±1 st. dev.

Conclusion

Under RCP8.5 scenario (and similarly in RCP2.6), nearly 12.7% (9.6% of global) of these areas show both increase in flood and drought risk. Unfortunately, these regions are the highly populated parts of the globe, the residence of around 30% of the world's current population, or more than 2.1 billion people. Simultaneous increases in drought and flood risks are largely projected to take place in less developed countries of Southeast Asia, Oceania and central Africa. These regions are more vulnerable to the threats arising from climate change compared to rich countries, as the majority of death toll from natural hazards reportedly correspond to the developing, low-income and middle-income countries.

A world 2°C warmer than the pre-industrial era will still face increases in flood and drought in most regions. However, the GCM and GHM ensemble shows that 4°C of warming will bring nearly twice as much increase and in a wider spread. The 2015 Paris Climate Agreement, adopted at COP21, targets to limit the global temperature rise "well below" 2°C above the pre-industrial levels. Even though seeming to be ambitious, such an agreement in intergovernmental level is a start to legally force the developed countries producing the majority of greenhouse gases to limit the emissions and finance the climate-resilient development in lower income economies.

Acknowledgement

The authors gratefully acknowledge support from NOAA under grants NA11SEC4810004, NA12OAR4310084, NA15OAR4310080 and PSC-CUNY Award # 68346-00 46. All statements made are the views of the authors and not the opinions of the funding agency or the U.S. government.